

See discussions, stats, and author profiles for this publication at: <https://www.researchgate.net/publication/225847810>

Size dependence of the superconducting critical temperature and fields of Nb/Al multilayers

Article in *Journal of Low Temperature Physics* · April 1986

DOI: 10.1007/BF00682068

CITATIONS

25

READS

23

6 authors, including:



Julio Guimpel

Centro Atómico Bariloche

125 PUBLICATIONS 2,177 CITATIONS

[SEE PROFILE](#)



Francisco de la Cruz

Centro Atómico Bariloche

174 PUBLICATIONS 3,158 CITATIONS

[SEE PROFILE](#)



Herman J Fink

University of California, Davis

118 PUBLICATIONS 1,580 CITATIONS

[SEE PROFILE](#)



Jean-Claude Villegier

Supratech Fr

190 PUBLICATIONS 2,466 CITATIONS

[SEE PROFILE](#)

Some of the authors of this publication are also working on these related projects:



JCV Josephson Circuits [View project](#)



Vortices in mesoscopic superconductors [View project](#)

Size Dependence of the Superconducting Critical Temperature and Fields of Nb/Al Multilayers

J. Guimpel, M. E. de la Cruz, and F. de la Cruz

Centro Atómico Bariloche, Bariloche, Argentina

H. J. Fink

Department of Electrical and Computer Engineering, University of California, Davis, California,
and Centro Atómico Bariloche, Bariloche, Argentina

O. Laborde

Centre de Recherches sur les Très Basses Températures, CNRS, Grenoble, France

J. C. Villegier

Laboratoire d'Electronique et de Technologie de l'Informatique, Centre d'Etudes Nucleaires de
Grenoble, Grenoble, France

(Received October 24, 1985)

The critical temperature T_c of Nb/Al multilayers decreases as the total sample thickness d_T is decreased while the thickness of each Nb and Al layer is kept constant. To understand this behavior, models based on the proximity effect and on weak two-dimensional (2D) localization are employed. The latter uses a characteristic length, the thermal diffusion length, in relation to d_T to obtain 2D behavior and leads to a reasonable explanation of $T_c(d_T)$. It is also found that the slope at $T_c(d_T)$ of the critical magnetic field perpendicular to the layers is independent of d_T when the Nb and Al layer thicknesses are kept constant. The angular dependence of the critical field is also measured.

1. INTRODUCTION

Metallic superlattices exhibit unique superconducting properties. Of particular interest to us are Nb thin films and superlattices with one component being Nb. For these, many observations are not understood or accounted for. Some of the results are the following.

Asada and Nose¹ measured the dependence of the superconducting transition temperature T_c of Nb on the film thickness d_T . They also measured the critical magnetic fields perpendicular H_{\perp} and parallel H_{\parallel} to the films. Their experimental results were interpreted¹ in terms of the oxidation and

columnar growth of the evaporated films. The H_{\perp} and H_{\parallel} experimental results did not fit the expected universal behavior.²

In rf sputtered Nb films it was also found^{3,4} that T_c decreases with decreasing film thickness. In Ref. 3 the normal and superconducting properties of Nb films were found to be very reproducible, indicating the high quality of their samples. The observed thickness dependence of T_c was explained^{3,5} in terms of the proximity effect induced by an intrinsic surface layer of thickness of the order of the interatomic distance. No critical field measurements were published for these samples.

In Nb-based multilayer structures⁶⁻¹² it is found that the critical temperature depends on the physical properties of the second component. Ruggiero *et al.*⁶ studied sputtered Nb/Ge metal-semiconductor multilayers. It was noticed that T_c decreased with the Nb layer thickness d_{Nb} at constant Ge layer thickness d_{Ge} . The value of T_c also decreased when d_{Ge} was increased at constant d_{Nb} . It is important to remark that the decrease of T_c for $d_{\text{Ge}} = 100 \text{ \AA}$ followed quantitatively the results found^{3,4} for isolated sputtered Nb films. The explanation of this result is based⁶ on the low electrical conductivity of Ge, which cannot induce changes in T_c according to the usual proximity effect theories. What is not clear to us concerning these results is the origin of the decrease of T_c in isolated Nb films, since the proximity effect invoked in Ref. 3 is not the same as that proposed⁶ in the Nb/Ge interface. The increase of T_c as d_{Ge} is decreased has no conclusive explanation.⁶

For Nb/Zr multilayers, Lowe and Geballe⁷ explain the change of T_c as a function of the period of the superlattice in terms of the proximity effect in a trilayer system of Nb/Nb-Zr alloy/Zr.

The behavior of the Nb/Cu multilayer system has been thoroughly investigated by Schuller and collaborators.⁸⁻¹² They found it impossible to explain the change in T_c as a function of the superlattice period d using the proximity effect calculations between Nb and Cu. As in the previous cases, the decrease of the critical temperature was stronger^{9,11} than expected. To explain their experimental data, it was assumed^{9,11} that the significant parameters of Nb should not be those of bulk Nb, but rather those that determine the T_c value of an isolated layer of thickness d_{Nb} . In this modified proximity effect picture the analysis of the data provided the relation between T_c of a single Nb layer and its thickness.

Although all results show a decrease of T_c with d_{Nb} , it was remarked¹¹ that there is no quantitative agreement among different authors, indicating the lack of a universal relationship. It was suggested¹¹ that the decrease in T_c is due to a decrease in the electronic mean free path $emfp$ and, in the case of thin films, the formation of a metallic surface layer which reduces T_c by means of the proximity effect.³

The interest in superconducting multilayers is not only limited to the change of the critical temperature. It is often assumed that a multilayer system can be treated within the framework of an anisotropic Ginzburg-Landau theory.¹³ This theory predicts an anisotropic bulk critical field with a well-characterized angular dependence. As in any mean field theory, its validity requires that the order parameter changes slowly within the characteristic distance of the problem. In the multilayer system the condition is that the perpendicular coherence length ξ_{\perp} should be larger than the lattice period. When this condition is not fulfilled, the theory breaks down.¹⁴ The behavior predicted by the mean field theory¹³ and the change in regime¹⁴ have been clearly seen in many samples by measuring the temperature dependence of the critical fields.^{6,10-12}

With these ideas in mind, we present the experimental results of Nb/Al multilayers as a function of total sample thickness d_T for constant Nb and Al layer thickness. Our results show that d_T determines the critical temperature of the multilayer system, as it does in pure Nb films.

2. SAMPLE PREPARATION AND EXPERIMENTAL TECHNIQUE

The Nb/Al multilayers were prepared by dc magnetron sputtering on a variety of substrates: Si (100), SiO₂, sapphire, and resist coated sapphire. Deposition rate was 15 Å/sec for Ar pressure of 15 mTorr. The residual gas pressure was 10⁻⁷ Torr. X-ray diffraction and XPS have been used to investigate the structure of the samples.¹⁵ Modulation thickness was measured directly by TEM and X-ray analysis. A coherent growth of (111) Al planes superimposed on (100) Nb planes was observed, with an interplane distance of 2.33 Å and a transverse grain size of about the sample thickness.¹⁵

Variation of the sample thickness was obtained by "peeling" layer by layer using a selective etching technique. Nb was selectively etched on Al by reactive ion etching with SF₆ gas, while Al films were dissolved by HCl solution. The end of the etching of each layer was controlled by *in situ* resistance measurements.

It was pointed out¹⁵ that the selective etching does not affect the structure of the remaining layers. It was also concluded¹⁵ that there existed a 15 Å interface of composition NbAl_x ($x \approx 2$). This interface is quite similar to the one observed by McWhan *et al.*¹⁶

Conventional ⁴He cryostats were used. The magnetic field was provided by a superconducting magnet or by a rotating iron magnet. Resistive superconducting transitions were measured with a conventional four-probe ac method. The transition temperature T_c and the critical fields were defined as those corresponding to resistance equal to 50% of the normal-state value.

The angle for the parallel and perpendicular critical fields was determined to 1 deg accuracy when using the superconducting magnetic and to 0.25 deg when using the rotating iron magnet.

In this paper we mainly report results for Nb/Al multilayers of 120 Å period with $d_{\text{Nb}} = d_{\text{Al}} = 60$ Å and different numbers of layers. However, data on samples of 47 and 60 Å period are also reported. For all samples $d_{\text{Nb}} = d_{\text{Al}} = d/2$.

3. EXPERIMENTAL RESULTS AND DISCUSSION

3.1. Critical Temperature and Resistivity

The experimental results for the critical temperature and resistivity are given in Table I. Figure 1 shows the measured critical temperature of our Nb/Al multilayers as a function of the inverse sample thickness d_T for Nb and Al layers of equal thickness, 60 Å. For comparison, the experimental results for Nb films of Refs. 1, 3, and 4 are also shown. The T_c values of our Nb/Al multilayers follow the same general trend as found for Nb films. This behavior cannot be explained in terms of the proximity effect between Nb and Al layers, because these were unchanged in the total sample thickness variation.

First, we investigate the influence of the proximity effect on the transition temperature of an infinite multilayer, then we compare our data to

TABLE I
Experimental Data of the Nb/Al Multilayer Samples^a

d , Å	d_T , Å	T_c , K	$\rho(10 \text{ K})$, $\mu\Omega\text{-cm}$	$\rho(300 \text{ K})$, $\mu\Omega\text{-cm}$	$(dH_{\perp}/dT)_{T_c}$, kOe/K
120	540	6.08	19.1	27.0	—
120	540	6.10	20.5	—	3.95
120	480	5.75	19.9	27.8	—
120	420	4.40	24.0	30.7	—
120	420	4.86	21.7	—	3.95
120	360	—	26.0	32.2	—
120	360	4.82	25.0	—	4.30
120	360	4.89	23.0	32.0	3.95
120	300	4.03	23.2	29.2	3.82
120	240	2.67	30.6	36.7	—
60	900	6.82	16.3	26.5	5.05
47	470	3.26	95.6	99.9	9.78
47	235	2.59	98.9	101.9	10.46

^a d , Period; d_T , total sample thickness; T_c , superconducting critical temperature; ρ resistivity, at 10 and 300 K; and $(dH_{\perp}/dT)_{T_c}$, slope of the perpendicular critical field at T_c ; in all samples the layer thickness, for both Nb and Al, is equal to half the period.

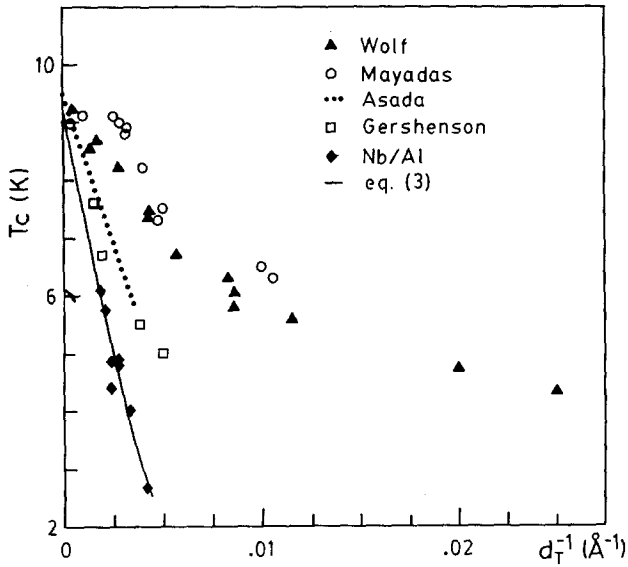


Fig. 1. Superconducting critical temperature T_c of the 120-Å-period Nb/Al multilayer samples as a function of the inverse of the total sample thickness d_T . (—) A fit of Eq. (3) to the experimental data with the hypothesis discussed in the text, $a = 65 \text{ \AA}$, $NV = 0.3063$, and $T_{SN} = 9.22 \text{ K}$. Data for Nb films from refs. 1, 3, and 4 are included.

mechanisms suggested in Ref. 3, which are made responsible for the strong thickness dependence of the transition temperature, and finally we interpret our data according to the spirit, but not the letter, of the weak localization theory of Fukuyama¹⁷ for two-dimensional superconductors.

3.1.1. Proximity Effect

If we apply the BCS formula, the transition temperature T_{SN} of an infinite multilayer system is given by

$$T_{SN} = (\theta_D/1.45) e^{-1/NV} \quad (1)$$

where we interpret θ_D as some average Debye temperature of the superlattice and NV as an effective coupling term. The former is usually assumed to be the arithmetic average of the Debye temperatures of the individual component materials and the latter is assumed to be given by an expression for a double layer by Cooper¹⁸ and slightly modified by de Gennes.¹⁹ In the dirty limit

$$NV = \frac{[N^2(0)Vd]_1 + [N^2(0)Vd]_2}{[N(0)d]_1 + [N(0)d]_2} \quad (2)$$

where subscripts 1 and 2 refer to the two component materials, $N(0)$ is the one-spin electronic density of states at the Fermi level, V is the BCS electron-electron interaction constant, and d is the layer thickness. Equation (2) does not take into account contributions from interface layers due to component alloying, and in our case is independent of the layer thickness, since $d_1 = d_2$. With the data shown in Table II and Eqs. (1) and (2) we obtain $T_{SN} = 9.22$ K. We interpret this value as the bulk transition temperature of a Nb/Al multilayer specimen. Thus, the proximity effect has a small influence on reducing the transition temperature of Nb compared to the observed reduction of T_c with d_T (Fig. 1). The calculated value of T_{SN} is in reasonable agreement with the extrapolation of the experimental data in the limit $d_T \rightarrow \infty$.

It should be mentioned that the proximity effect theory had been employed previously to explain^{6,7} the change of the transition temperature of multilayers of Nb/Zr and Nb/Ge, and in a modified fashion to explain^{9,11} the size effect of the Nb layers in Nb/Cu periodic structures.

As shown above, the proximity effect in Nb/Al double layers has a relatively small effect in changing $T_c(d_T)$. We believe this is why we could not detect, within our experimental accuracy, oscillations in $T_c(d_T)$ when the number of layers in our specimens was varied between odd and even.

3.1.2. Metallic Surface Layer

In Ref. 3 it was argued that the decrease of T_c with decreasing d_T was due to the proximity effect of a surface layer of unknown origin. This overlay becomes most effective in reducing T_c if it is a normal metal with $V = 0$. With this hypothesis and the application of Eq. (2) extended to a trilayer system, the transition temperature becomes

$$T_c(d_T) = T_{SN} \exp \left\{ -\frac{a}{d_T - a} \frac{2N_a(0)}{NV[N_1(0) + N_2(0)]} \right\} \quad (3)$$

TABLE II

Proximity Effect Calculation of the Superconducting Critical Temperature of an Infinite Nb/Al Multilayer for Equal Nb and Al Layer Thickness

Material	$N(0)$, 10^{23} states/eV cm^3 spin	θ_D , K	T_c , K	NV
Nb	0.90 ^a	277 ^a	9.26 ^a	0.3304 ^b
Al	0.174 ^a	423 ^a	1.196 ^a	0.1819 ^b
Nb/Al ($d_{Nb} = d_{Al}$)	—	350 ^c	9.22 ^b \pm 1 ^d	0.3063 ^e

^aFrom ref. 24.

^bCalculated from the BCS equation for T_c .

^c $(\theta_D^{Nb} + \theta_D^{Al})/2$.

^dRepresents the dispersion when using data from different authors.

^eCalculated from Eq. (2).

where a is the surface layer thickness and $N_a(0)$ is the one-spin electronic density of states of this layer. Equation (3) can be fitted to our data with $a = 65 \text{ \AA}$ assuming $N_a(0) = [N_1(0) + N_2(0)]/2$.

In Fig. 2 we show the residual resistivity ρ at 10 K of the Nb/Al multilayers as a function of inverse sample thickness. A similar behavior has been found^{1,4} in the resistivity of Nb single films. The dashed line represents a linear fit to the data. If the overlay is a metal with the same resistivity as the multilayer, then the resistivity of the specimen should not vary with d_T . This is shown by the horizontal line in Fig. 2. On the other hand, if the overlay of thickness $a = 65 \text{ \AA}$ is a worse conductor than the multilayer, then the total resistivity of the specimen should vary at most [in the limit $N_a(0) = 0$] as shown by the solid curve in Fig. 2. In this limit $T_c(d_T)$ should not vary at all due to the proximity effect of the overlay. It is clear that with the results obtained in the fit of Eq. (3) to our T_c data, we cannot explain our resistivity data. It will be shown in the next section that the variation of ρ with d_T cannot be due to a change in the electronic diffusion constant D , since it is found to be independent of d_T . We therefore rule out the possibility that the proximity effect of an overlay can take into account the drastic variation of T_c with d_T shown in Fig. 1 and the observed change in ρ .

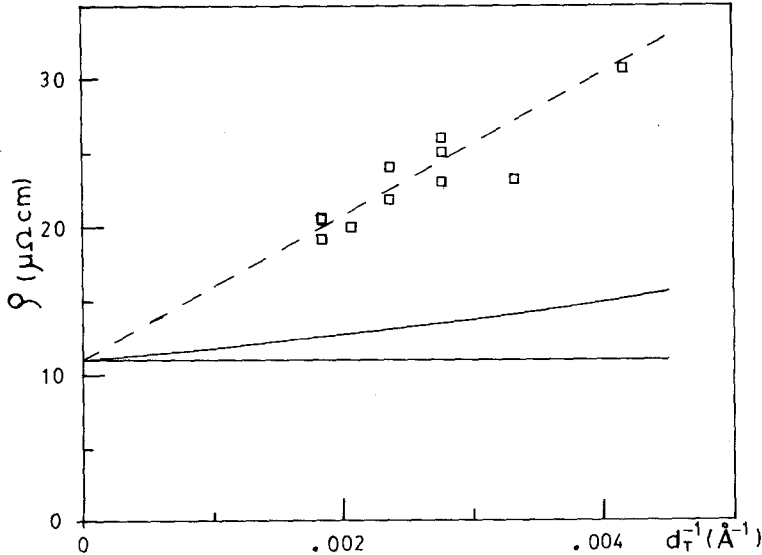


Fig. 2. Residual resistivity $\rho(10 \text{ K})$ of the 120- \AA -period Nb/Al multilayer samples as a function of the inverse of the total sample thickness. (---) A linear fit to the data; (—) the effect of a 65- \AA surface layer in the limits where it has the same resistivity as the multilayer and where it is an insulator.

Since the increase of the resistivity is not due to a variation of D , one might intuitively conjecture that the change in T_c is directly related to that of ρ . However, the following discussion will show that there are no straightforward arguments relating the behavior of both quantities.

3.1.3. Weak Localization-2D Effects

Here we attempt to elucidate our $T_c(d_T)$ results in the spirit of Fukuyama *et al.*'s theory of weak localization¹⁷ and their two-dimensional (2D) corrections. Unfortunately, the numerical results¹⁷ apply to single, high-resistivity, uniform films, not to multilayers. Therefore we do not expect numerical agreement. However, in the spirit of this theory one can write¹⁷

$$T_c(d_T) = T_{c0} e^{-K_3} e^{-K_2} \quad (4)$$

where T_{c0} is the critical temperature of the bulk material without localization effects and K_3 takes account of the bulk quantum corrections to T_c due to localization.²⁰ The K_2 term is due to electron diffusion processes, which can be viewed as essentially 2D if $l_{th} > d_T$, where $l_{th} = (\hbar D/kT)^{1/2}$ is the thermal diffusion length.¹⁷ The K_2 must scale¹⁷ as l_{th}/d_T . The quantum corrections to T_c then have a 2D character, although the parameters describing the electrons are of 3D nature.

Applying Eq. (4) to our multilayers, we interpret T_{c0} as the bulk effective critical temperature T_{SN} . The K_2 is replaced by

$$K_2 \equiv \frac{l_{th}}{d_T} = \frac{1}{d_T} \left(\frac{\hbar D}{kT_c} \right)^{1/2} \quad (5)$$

where T has to be replaced by $T_c(d_T)$ in l_{th} when used in conjunction with Eq. (4). Then Eq. (4) becomes

$$T_c(d_T) = T_\infty \exp \{ -\alpha/d_T [T_c(d_T)]^{1/2} \} \quad (6)$$

where $T_\infty = T_{SN} \exp(-K_3)$ and $\alpha^2 = \hbar D/k$. The T_∞ includes both proximity and 3D localization effects. Figure 3 shows the best fit of Eq. (6) to the experimental data. The values of T_∞ and D obtained in such a way are 8.25 K and 2.59 cm²/sec, respectively. It will be shown below that D , obtained independently from critical field measurements, has a value of 2.74 cm²/sec, which compares favorably with the above value. This leads us to believe that Eq. (6) correctly describes our data and that the fundamental characteristic length for the determination of the critical temperature in our multilayer specimens is the thermal diffusion length.

Unfortunately, we have not been able to find such a simple way to analyze the resistivity data of multilayers in this weak localization

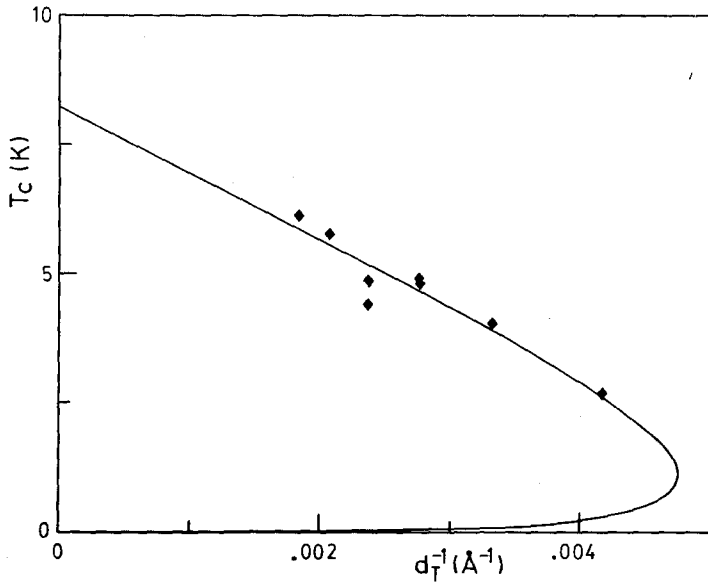


Fig. 3. Superconducting critical temperature T_c of the 120- \AA -period Nb/Al multilayer samples as a function of the inverse of the total sample thickness d_T . (—) The modified Fukuyama expression,¹⁷ Eq. (6), with $T_\infty = 8.25$ K and $D = 2.59$ cm^2/sec .

framework. As a consequence, the thickness dependence of ρ remains an open question.

3.2. Critical Magnetic Fields

3.2.1. Perpendicular Critical Field

Figure 4a shows the experimental results for H_\perp as a function of temperature for samples with $d_{\text{Nb}} = d_{\text{Al}} = 60$ \AA and $d_T = 300, 360, 420,$ and 540 \AA . Figure 4b shows similar results for samples with $d_{\text{Nb}} = d_{\text{Al}} = 23$ and 30 \AA . One can observe that within the experimental accuracy $(dH_\perp/dT)_{T_c}$ remains constant for constant layer thickness when the total sample thickness is varied (see Table I). It is also observed that for smaller layer thickness $(dH_\perp/dT)_{T_c}$ becomes steeper.

Let us consider the relation between H_\perp and the electronic diffusion constant D , which we have used in discussing the thickness dependence of T_c . In an anisotropic Ginzburg-Landau theory¹³

$$H_\perp = \phi_0 / 2\pi\xi_\parallel^2(t) \quad (7)$$

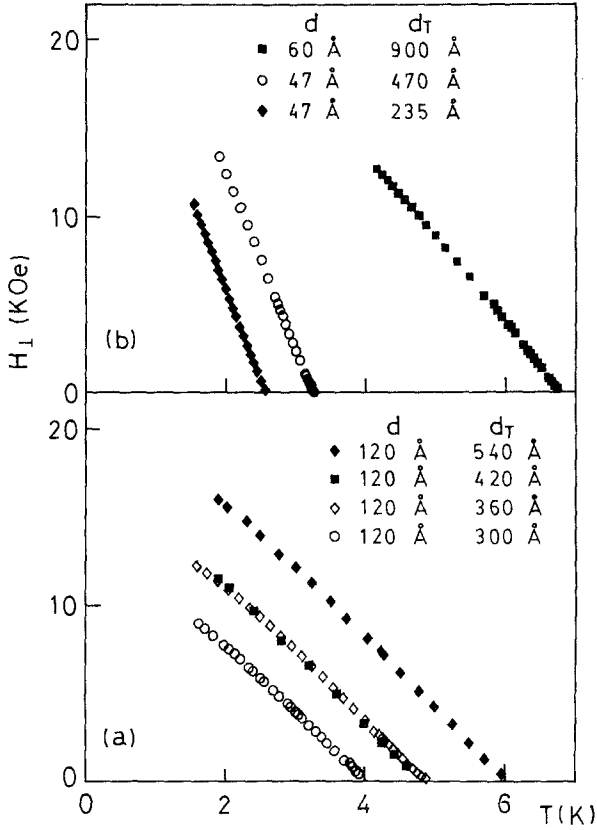


Fig. 4. Perpendicular critical field H_{\perp} as a function of temperature for Nb/Al multilayers of (a) period 120 Å, (b) period 60 and 47 Å.

where ϕ_0 is the flux quantum, ξ_{\parallel} is the coherence length in the direction parallel to the layers, and $t = T/T_c$ is the reduced temperature. For our specimens one estimates the elastic emfp to be smaller than the period $d = d_{\text{Nb}} + d_{\text{Al}}$. It is probably limited to a large extent by the Nb and Al layer thickness. It is therefore appropriate to interpret ξ_{\parallel} to be in the dirty limit ($l < \xi_0$). Since in Eq. (7) $\xi_{\parallel}(t)$ is a parameter that describes collectively the properties of the Nb/Al multilayer, it stands to reason that the parameters that define it must also be collective. Then

$$\xi_{\parallel}^2(t) = \frac{\pi}{8} \left(\frac{\hbar D}{kT_c} \right) \frac{1+t^2}{1-t^2} \quad (8)$$

where D is an effective diffusion constant for the Nb/Al multilayer.

Combining Eqs. (7) and (8), we get

$$\left(\frac{dH_{\perp}}{dT}\right)_{T_c} = \frac{4}{\pi} \frac{ck}{e} \frac{1}{D} \quad (9)$$

Equation (9) is in cgs gaussian units. The constancy of $(dH_{\perp}/dT)_{T_c}$ indicates that D remains constant as the sample thickness d_T is changed at constant Nb and Al layer thickness. The value of D obtained from Eq. (9) for the $d = 120 \text{ \AA}$ samples, $2.74 \text{ cm}^2/\text{sec}$, agrees with that obtained from the T_c data through Eq. (6). In a homogeneous material the electronic diffusion constant is $D = v_F l/3$, where v_F is the Fermi velocity and l is the emfp. Since $D^{-1} = 2 e^2 N(0) \rho$, a decrease in T_c together with an increase in ρ at constant D can be associated with a decrease in $N(0)$. On the other hand, for a nonhomogeneous superconductor the D in Eq. (9) represents some average that takes into account the transport properties of each component material and the electron scattering at the interfaces between layers. The constancy of $(dH_{\perp}/dT)_{T_c}$ in our multilayers provides experimental evidence that the technique used to reduce d_T does not affect the diffusion constant. As a consequence, the change in $\rho(d_T)$, Fig. 2, cannot be readily understood in terms of a change in the emfp. In relation to this, the results of Ref. 21 are of interest. It is shown²¹ that addition of O up to 2% to pure Nb decreases T_c to about 7 K and increases $(dH_{c2}/dT)_{T_c}$ by a factor of four. Again the constancy of the slope of the perpendicular critical field in our samples indicates that the thickness dependence of T_c cannot be due to an increase in the O concentration.

3.2.2. Parallel Critical Field

One can easily imagine that multilayer specimens will show anisotropic properties in the critical magnetic fields. Within the framework of a mean field theory¹³ the concept of the anisotropic coherence lengths ξ_{\parallel} and ξ_{\perp} are introduced. The parallel critical field is then

$$H_{\parallel} = b\phi_0/2\pi\xi_{\parallel}(t)\xi_{\perp}(t) \quad (10)$$

where $b = 1$ for the anisotropic bulk critical field and $b = 1.695$ for the parallel surface nucleation field.¹³ Size effect anisotropy should also appear when $d_T \leq \xi_{\perp}$. In this thin limit H_{\parallel} becomes²²

$$(H_{\parallel}/H_r)^2 = 12H_{\perp}/H_r \quad (11)$$

with $H_r = \phi_0/(2\pi d_T^2)$ being a normalization field. It is interesting to remark that Eq. (11) is the same as that for an isotropic specimen² with $\xi = \xi_{\parallel}$. This is due to the fact that the only anisotropy remaining in this limit has a geometrical origin; ξ_{\perp} has been replaced by d_T and determines the range of variation of the order parameter in the direction perpendicular to the multilayer.

Figure 5 shows the experimental results for H_{\parallel} as a function of temperature. The solid lines are calculated for each sample in the thin limit from the experimental result of H_{\perp} and Eq. (11), and in the thick limit by arbitrarily putting $\xi_{\perp} = \xi_{\parallel}$ [obtained from H_{\perp} and Eq. (7)] together with $b = 1.695$ in Eq. (10). We see that the agreement between the experimental data and Eq. (11) is excellent, without adjustable parameters, for the thinner specimens. In the thicker limit the temperature dependence of the experimental data is not understood and does not represent the typical transition from the thin-limit behavior near T_c [$H_{\parallel} \propto (1-t)^{1/2}$] to the thick-limit behavior [$H_{\parallel} \propto (1-t)$].

On the other hand, the angular dependence of the critical field (Fig. 6) follows, for all samples and temperatures, Tinkham's theory²³ for isotropic

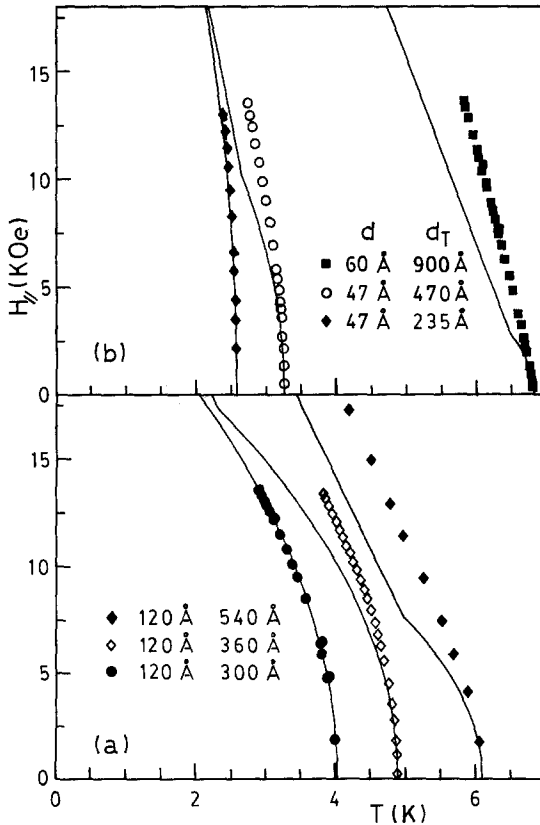


Fig. 5. Parallel critical field H_{\parallel} as a function of temperature for Nb/Al multilayers of (a) period 120 Å, (b) period 60 and 47 Å.

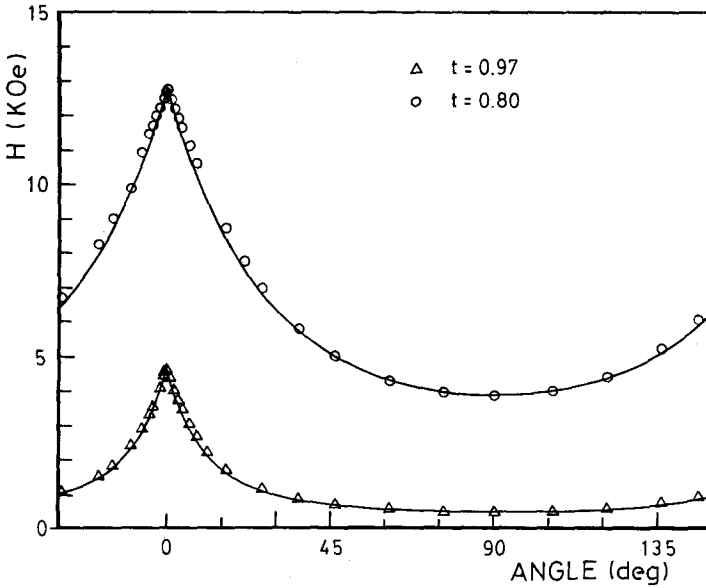


Fig. 6. Angular dependence of the critical field of the Nb/Al multilayer sample of period 120 \AA and total thickness 360 \AA at two reduced temperatures ($T_c = 4.89 \text{ K}$). (—) The fit to Tinkham's theory.

superconductors. For H almost parallel to the same surfaces, sharp cusps are always observed.

4. CONCLUSIONS

We have experimentally shown that the critical temperature of thin films of Nb/Al multilayers depends on the thickness of the sample, and follows a similar trend as that observed in pure Nb films.^{1,3,4}

The slope of the perpendicular critical field at T_c does not depend on d_T for fixed Nb and Al layer thickness, which indicates that the electronic diffusivity of the multilayer is not modified by d_T . As a consequence, the change in the resistivity is not due to a modification of the emfp, but rather to the variation of a properly averaged density of states. At the present time there is no theory relating the multilayer resistivity and effective BCS electron-electron interaction with adequate averages of the density of states and diffusion coefficients of the component materials. Nevertheless, our results strongly suggest that the decrease in T_c should be directly related to the increase in ρ .

The experimental results for T_c as a function of d_T can be fitted by a theoretical expression taking into account the proximity effect between the

multilayer and a surface layer, but the model fails when used to explain the increase in ρ .

Since the thermal electron diffusion length of our films is of the order of d_T , we have used Fukuyama's¹⁷ ideas to suggest that the decrease in T_c could be due to 2D weak localization effects. Although the qualitative agreement has been found to be very good, a quantitative check has to wait until the theory is extended to nonhomogeneous materials.

Finally, we remark that whichever is the microscopic mechanism that determines the dependence of T_c on d_T for single Nb films, it is present in our Nb/Al multilayers. Our results show that a distance much larger than the period of the superlattice is the characteristic length for the critical temperature variation, indicating the existence of some sort of coherence that is not broken by the interface between layers.

ACKNOWLEDGMENTS

We thank J. Simonin for helpful discussions. One of the authors (H.J.F.) thanks Dr. H. Fukuyama for correspondence.

This work was partially supported by the Organization of American States through the Multinational Program in Physics and by the French-Argentinian cooperation program.

H.J.F. was supported in part by NSF grant INT-8502375. J.G. was a recipient of a fellowship granted by the Comisión Nacional de Energía Atómica (CNEA). The Centro Atómico Bariloche is affiliated with the CNEA.

REFERENCES

1. Y. Asada and H. Nose, *J. Phys. Soc. Japan* **26**, 347 (1969).
2. D. Saint-James and P. G. de Gennes, *Phys. Lett.* **7**, 306 (1963).
3. S. A. Wolf, J. J. Kennedy, and M. Nisenoff, *J. Vac. Sci. Technol.* **13**, 145 (1976).
4. A. F. Mayadas, R. B. Laibowitz, and J. J. Cuomo, *J. Appl. Phys.* **43**, 1287 (1972); M. E. Gershenson and V. N. Gubankov, *Physica* **108B+C**, 971 (1981).
5. J. Simonin, in *Proc. 9° Simposio Latinoamericano de Fisica del Estado Solido* (Mar del Plata, Argentina, 1985), p. 164.
6. S. T. Ruggiero, T. W. Barbee, Jr., and M. R. Beasley, *Phys. Rev. Lett.* **45**, 1299 (1980); *Phys. Rev. B* **26**, 4894 (1982).
7. W. P. Lowe and T. H. Geballe, *Phys. Rev. B* **29**, 4961 (1984); T. Claeson, J. B. Boyce, W. P. Lowe, and T. H. Geballe, *Phys. Rev. B* **29**, 4969 (1984).
8. I. K. Schuller, *Phys. Rev. Lett.* **44**, 1597 (1980).
9. I. Banerjee, Q. S. Yang, C. M. Falco, and I. K. Schuller, *Solid State Commun.* **41**, 805 (1982).
10. I. Banerjee, Q. S. Yang, C. M. Falco, and I. K. Schuller, *Phys. Rev. B* **28**, 5037 (1983).
11. I. Banerjee and I. K. Schuller, *J. Low Temp. Phys.* **54**, 501 (1984).
12. C. S. L. Chun, G.-G. Zheng, J. L. Vicent, and I. K. Schuller, *Phys. Rev. B* **29**, 4915 (1984).
13. D. R. Tilley, *Proc. Phys. Soc.* **85**, 1177 (1965); W. E. Lawrence and S. Doniach, in *Proceedings of the 12th International Conference on Low Temperature Physics*, E. Kanda, ed. (Academic Press of Japan, Kyoto, 1971), p. 361.

14. R. A. Klemm, A. Luther, and M. R. Beasley, *Phys. Rev. B* **12**, 877 (1975); G. Deutscher and O. Entin-Wohlman, *Phys. Rev. B* **17**, 1249 (1978).
15. J. C. Villegier, B. Blanchard, and O. Laborde, in *Proceedings of the 17th International Conference on Low Temperature Physics*, U. Eckern, A. Schmid, W. Weber, and H. Wühl, eds. (North-Holland, Amsterdam, 1984), p. 233.
16. D. B. McWhan, M. Gurvitch, J. M. Rowell, and L. R. Walker, *J. Appl. Phys.* **54**, 3886 (1983).
17. H. Fukuyama, *Physica* **126B**, 306 (1984); H. Ebisawa, H. Fukuyama, and S. Maekawa, *J. Phys. Soc. Japan* **54**, 2257 (1985).
18. L. N. Cooper, *Phys. Rev. Lett.* **6**, 689 (1961).
19. P. G. de Gennes, *Rev. Mod. Phys.* **36**, 225 (1964).
20. E. Abrahams, P. W. Anderson, D. C. Licciardello, and T. V. Ramakrishnan, *Phys. Rev. Lett.* **42**, 673 (1979).
21. W. DeSorbo, *Phys. Rev.* **132**, 107 (1963); C. C. Koch, J. O. Scarbrough, and D. M. Kroeger, *Phys. Rev. B* **9**, 888 (1974).
22. E. V. Minenko, *Sov. J. Low Temp. Phys.* **9**, 535 (1983).
23. M. Tinkham, *Phys. Rev.* **129**, 2413 (1963).
24. G. Gladstone, M. A. Jensen, and J. R. Schrieffer, in *Superconductivity*, R. D. Parks, ed. (Dekker, New York, 1969), p. 734.